



Original Contribution

Quantitation of mercapturic acid conjugates of 4-hydroxy-2-nonenal and 4-oxo-2-nonenal metabolites in a smoking cessation study

Heather C. Kuiper^a, Brandi L. Langsdorf^a, Cristobal L. Miranda^a, Jacqueline Joss^b, Carole Jubert^c, John E. Mata^c, Jan F. Stevens^{a,*}^a Linus Pauling Institute and the Department of Pharmaceutical Sciences, Oregon State University, Corvallis, OR 97331, USA^b Pharmacy Department, Good Samaritan Regional Medical Center, Corvallis, OR 97330, USA^c Department of Biomedical Sciences, Oregon State University, Corvallis, OR 97331, USA

ARTICLE INFO

Article history:

Received 11 July 2009

Revised 29 August 2009

Accepted 3 October 2009

Available online 9 October 2009

Keywords:

Lipid peroxidation

Quantitation

4-Hydroxy-2-nonenal

4-Oxo-2-nonenal

Mass spectrometry

Smoking

ABSTRACT

The breakdown of polyunsaturated fatty acids (PUFAs) under conditions of oxidative stress results in the formation of lipid peroxidation (LPO) products. These LPO products such as 4-hydroxy-2-nonenal (HNE) and 4-oxo-2-nonenal (ONE) can contribute to the development of cardiovascular and neurodegenerative diseases and cancer. Conjugation with glutathione, followed by further metabolism to mercapturic acid (MA) conjugates, can mitigate the effects of these LPO products in disease development by facilitating their excretion from the body. We have developed a quantitative method to simultaneously assess levels of 4-oxo-2-nonen-1-ol (ONO)-MA, HNE-MA, and 1,4-dihydroxy-2-nonene (DHN)-MA in human urine samples utilizing isotope-dilution mass spectrometry. We are also able to detect 4-hydroxy-2-nonenic acid (HNA)-MA, 4-hydroxy-2-nonenic acid lactone (HNAL)-MA, and 4-oxo-2-nonenic acid (ONA)-MA with this method. The detection of ONO-MA and ONA-MA in humans is significant because it demonstrates that HNE/ONE branching occurs in the breakdown of PUFAs and suggests that ONO may contribute to the harmful effects currently associated with HNE. We were able to show significant decreases in HNE-MA, DHN-MA, and total LPO-MA in a group of seven smokers upon smoking cessation. These data demonstrate the value of HNE and ONE metabolites as *in vivo* markers of oxidative stress.

© 2009 Elsevier Inc. All rights reserved.

Introduction

Oxidative degradation of polyunsaturated fatty acids (PUFAs) occurs under conditions of oxidative stress when the cellular antioxidant defense mechanisms are overwhelmed, leading to the formation of electrophilic lipid peroxidation (LPO) products. 4-Hydroxy-2-nonenal (HNE) and 4-oxo-2-nonenal (ONE) are two of the most thoroughly studied LPO products. These reactive aldehydes have been shown to be cytotoxic and genotoxic [1,2], as well as to contribute to the development and progression of cancer [3], cardiovascular diseases such as atherosclerosis and chronic obstructive pulmonary disease [4–6], and neurodegenerative diseases like Alzheimer's [7–9]. In biological systems, HNE and ONE undergo phase

I metabolism, resulting in their respective oxidation products 4-hydroxy-2-nonenic acid (HNA) [10] and 4-oxo-2-nonenic acid (ONA) [11] or reduction products 1,4-dihydroxy-2-nonene (DHN) [12] and 4-oxo-2-nonen-1-ol (ONO) [13–15] (Scheme 1). HNE, ONE, and their phase I metabolites have also been shown to undergo phase II metabolism, forming Michael-type conjugates with glutathione (GSH) [2], a reaction mediated by glutathione S-transferase (GST) [16–18]. On conjugation, HNA can form a lactone (HNAL) via spontaneous intramolecular condensation [19]. Further metabolism of these LPO-GSH conjugates in the liver and kidney results in LPO-mercapturic acid (MA) conjugates which are excreted in urine.

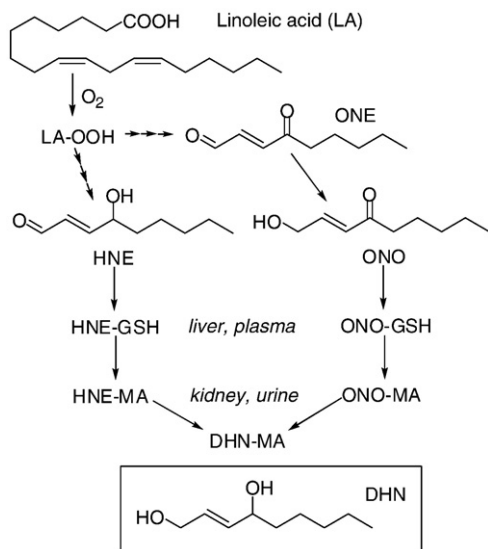
We have previously reported that HNE and ONE metabolite levels are significantly increased in rats after an acute oxidative stress insult [20]. In that study we were able to differentiate between HNE-MA and its isomer ONO-MA which had not been previously demonstrated. This is an important distinction because previous analyses have likely attributed the effects of ONO to HNE. These metabolites also form by different pathways, so being able to distinguish between the two could provide insight into the mechanisms of oxidative stress in biological systems. Previous studies have focused on the quantitation of DHN-MA [21–24].

Here we report the quantitation of HNE-MA and ONO-MA, as well as DHN-MA in human urine. The phase I metabolites of HNE-MA and ONE-MA represent biologically relevant pathways for the elimination

Abbreviations: BMI, body mass index; DHN, 1,4-dihydroxy-2-nonene; EPI, enhanced product ion; GSH, glutathione; GST, glutathione S-transferase; HNA, 4-hydroxy-2-nonenic acid; HNAL, 4-hydroxy-2-nonenic acid lactone; HNE, 4-hydroxy-2-nonenal; HPLC, high performance liquid chromatography; LC, liquid chromatography; LPO, lipid peroxidation; MA, mercapturic acid; MA₃, N-(acetyl-d₃)-L-cysteine; MS, mass spectrometry; ONA, 4-oxo-2-nonenic acid; ONE, 4-oxo-2-nonenal; ONO, 4-oxo-2-nonen-1-ol; PUFA, polyunsaturated fatty acid; SNP, single nucleotide polymorphisms; SRM, selected reaction monitoring; TOG, thiazadiazabicyclo-ONE-glutathione.

* Corresponding author. Oregon State University, 203 Pharmacy Building, 1601 SW Jefferson, Corvallis, OR 97331-3507, USA. Fax: +1 541 737 3999.

E-mail address: fred.stevens@oregonstate.edu (J.F. Stevens).



Scheme 1. LPO-induced degradation of linoleic acid. HNE and ONE undergo phase I and phase II metabolism, resulting in the excretion of MA conjugates including HNE-MA, ONO-MA, and DHN-MA. DHN-MA may originate from DHN-GSH, possibly via ONO-GSH, but DHN-MA is shown as a metabolite of HNE-MA and ONO-MA for simplicity.

of these LPO products in a rat model of oxidative stress [20]. We have detected HNE-MA, DHN-MA, HNA-MA, HNAL-MA, ONO-MA, and ONA-MA in human samples and are able to quantitate the HNE-MA, ONO-MA, and DHN-MA metabolites in smokers. Twelve weeks of smoking cessation resulted in a significant decrease in the levels of urinary HNE-MA, DHN-MA, and overall LPO-MA. These results demonstrate the potential utility of these metabolites as noninvasive diagnostic tools for assessing oxidative stress *in vivo*.

Materials and methods

Materials

[²H]Chloroform was purchased from Cambridge Isotope Laboratories (Andover, MA). HPLC-grade formic acid (0.1%) in water was purchased from Honeywell Burdick and Jackson (Muskegon, MI). 3-Chloroperoxybenzoic acid and dithiothreitol were purchased from TCI America (Portland, OR). HNE-MA (1 mg in 100 μ l ethanol) was purchased from Cayman Chemical (Ann Arbor, MI). Cotinine was purchased from Alfa Aesar (Ward Hill, MA) and cotinine-*d*₃ (99 atom % D, 1 mg/ml in methanol) was from Sigma-Aldrich (St. Louis, MO). All other chemicals were purchased from Sigma-Aldrich (St. Louis, MO).

Synthesis

LPO products

HNE, HNA, ONE, ONO, and ONA and their MA conjugates were prepared and chemically characterized as described in our previous work [20].

Deuterium-labeled MA

N-(acetyl-*d*₃)-L-cysteine (MAD₃) was prepared using the method of Slatter et al. [25]. Briefly, cystine (5.3 mmol) was added to 13 ml of a 1.5 M NaOH solution and the mixture was cooled in an ice bath with stirring. [²H₆]Acetic anhydride (10.6 mmol) was added dropwise over 20 min, the ice bath was removed, and the reaction continued with stirring at room temperature for 1 h. 1,4-Dithiothreitol (10.6 mmol) was added, and the reaction mixture was stirred continuously at room temperature for 1 h, concentrated *in vacuo*, washed with ether, frozen, and lyophilized. Purification was performed on a 52 \times 2.5-cm Sephadex LH-20 column using methanol as the eluting solvent.

Fraction purity was verified by LC-MS analysis in negative ion mode. Only fractions containing a peak at *m/z* 165 (MAD₃) were carried forward. Further purification was carried out by acidification to pH 3 with 1 M HCl and extraction with ethyl acetate, in order to remove any remaining cystine or cysteine. The organic layer was concentrated *in vacuo*. The resulting white residue was characterized by LC-MS/MS analysis and found to be free of cystine, cysteine, and unlabeled mercapturic acid.

Preparation of LPO-MAD₃ conjugates

MAD₃ was used in place of MA for LPO-MA adduct formation [20] for use as internal standards. Briefly, a 20 mM solution of MAD₃ was prepared in 0.1 M sodium phosphate buffer, pH 8. To 50 μ l of this solution was added 450 μ l of the same phosphate buffer and 400 μ l of water. A 1.0 mM solution of the LPO product of interest was made up in ethanol and 100 μ l was added to the MAD₃ solution (10-fold molar excess). The reaction was stirred at 37 $^{\circ}$ C for 2 h and then acidified to pH 3 with 1 N HCl. It was then extracted with ethyl acetate, 3 \times 1 ml, evaporated under nitrogen using a Zymark TurboVap LV (Caliper Life Sciences, Hopkinton, MA), and reconstituted in 1.0 ml of 2:8 acetonitrile-H₂O containing 0.1% formic acid, yielding a nominal LPO-MAD₃ concentration of 100 μ M. LC-MS/MS analyses were used to verify conjugate formation.

Sample collection

This study protocol No. 4312 was approved by Oregon State University's and Samaritan Health Systems' Institutional Review Boards. Participants were recruited by newspaper advertisements in the Corvallis, Oregon, area. Participants who responded were enrolled because they met our study participation criteria: age 18–65 years, healthy, current smoker motivated to quit for one arm of the study, nonsmoker with minimal exposure to second-hand smoke in the control group, BMI <35 kg/m², subjects may not be taking any prescription, no over-the-counter or herbal medications that induce or inhibit the liver enzymes involved in drug metabolism (CYP P450 3A4, 2D6), no known active liver disease (hepatitis, cirrhosis), no excessive alcohol use defined as >1 drink per day for women and >2 drinks per day for men. Nonsmokers were enrolled into the study and matched by age and BMI to one of the smokers already enrolled in the study (Table 1). Each subject signed an informed consent statement and completed a questionnaire that provided the following information: age, sex, weight, height, history of tobacco use, and health status prior to enrollment in the study.

Urine samples were collected from smokers and nonsmokers at Good Samaritan Hospital (Corvallis, OR). On the day of the study, 23 smokers and 23 nonsmokers provided at least 10 ml of clean catch urine. A second urine sample was collected at least 12 weeks after smoking cessation from the seven smokers who successfully quit smoking and their nonsmoking counterparts. On collection, samples were frozen and stored at -80 $^{\circ}$ C until analysis. Smoking cessation was carried out using either Chantix (varenicline tartrate, which blocks nicotine receptors in the brain), Zyban (bupropion hydrochloride,

Table 1
Study participant characteristics

Parameter	All enrolled participants		Cessation study ^b	
	Nonsmokers (n = 23)	Smokers (n = 23)	Nonsmokers (n = 7)	Smokers (n = 7)
Gender ^a	10 Male, 13 Female	9 Male, 14 Female	4 Male, 3 Female	4 Male, 3 Female
Age (years) ^a	42.7 \pm 12.0	42.5 \pm 10.8	37.4 \pm 10.7	38.7 \pm 8.6
BMI (kg/m ²) ^a	26.8 \pm 4.5	27.0 \pm 4.6	25.9 \pm 4.1	26.0 \pm 4.1
Years smoked	0	19.5 \pm 12.5	0	16.2 \pm 7.5

^a No significant difference between the two groups.

^b Nonsmokers were matched by age and BMI to one of the smokers.

presumably acting by modulation of noradrenergic and dopaminergic receptors in the brain), or quitting “cold turkey.” Support was provided during the cessation process through a smoking cessation class and phone calls. Self-reporting and cotinine levels were used to verify the success of smoking cessation.

Urine samples

A volume of 0.2 ml of human urine was acidified with 20 μ l of 1 N HCl to pH 3. To the urine was added 5 μ l of a 100 μ M solution of DHN-MAd₃, 10 μ l of a 10 μ M solution of HNE-MAd₃, and 10 μ l of a 10 μ M solution of ONO-MAd₃ as internal standards. The samples were extracted with ethyl acetate (2 \times 700 μ l). The ethyl acetate layers were combined and evaporated under nitrogen. Samples were then reconstituted in 100 μ l of 2:8 acetonitrile:water containing 0.1% formic acid and analyzed by LC-MS/MS.

Urinary creatinine was measured using a Creatinine Assay Kit, Catalog No. 500701 (Cayman Chemical). The assay was performed according to the manufacturer's directions. There was no significant difference between smoker and nonsmoker creatinine levels ($P=0.37$).

Urinary cotinine was analyzed by LC-MS/MS. To a volume of 0.2 ml of human urine was added 5 μ l of 10 μ M cotinine-d₃ as an internal standard. Proteins were precipitated by the addition of 795 μ l of MeCN containing 0.1% formic acid and centrifugation. The supernatant was analyzed by LC-MS/MS.

Calibration curves

A calibration curve was constructed from standard solutions of HNE-MA, DHN-MA, and ONO-MA in 2:8 acetonitrile:water (both with 0.1% formic acid). The ONO-MA concentrations ranged from 10 nM to 1.0 μ M and included six points, while the DHN-MA and HNE-MA concentrations ranged from 50 nM to 5.0 μ M and included seven points. HNE-MAd₃ (10 μ l of a 10 μ M solution), DHN-MAd₃ (5 μ l of a 100 μ M solution), and ONO-MAd₃ (10 μ l of a 10 μ M solution) were added as internal standards. The final volume of each standard solution was 100 μ l.

A second calibration curve was prepared for the analysis of urinary cotinine. The curve, prepared in ethanol, included seven points with concentrations ranging from 0.1 nM to 1 μ M. Cotinine-d₃ (5 μ l of 10 μ M) was used as the internal standard.

Standard addition curves

The standard addition curves were prepared by adding synthetic HNE-MA, DHN-MA, or ONO-MA and the corresponding internal standard to urine samples. One-milliliter aliquots of urine were used for each point on the curve. The urine was acidified to pH 3 with 1 N HCl and spiked with varying concentrations of HNE-MA (0.5–5.0 μ M), DHN-MA (0.1–5.0 μ M), or ONO-MA (0.25–1.0 μ M) and a fixed amount of internal standard, i.e., HNE-MAd₃ (20 μ l of a 10 μ M solution), DHN-MAd₃ (10 μ l of a 100 μ M solution), or ONO-MAd₃ (20 μ l of a 10 μ M solution). Samples were then vortex-mixed and extracted with ethyl acetate (2 \times 2 ml). The combined ethyl acetate layers were evaporated under N₂ and reconstituted in 200 μ l of 2:8 acetonitrile:water containing 0.1% formic acid.

HPLC

A Shimadzu Prominence HPLC system (Shimadzu, Columbia, MD) consisting of four LC-20AD pumps, a DQU-20A₅ degasser, and an SIL-HTc autosampler, equipped with switching valves, was used for all chromatography. For LPO product analyses, the HPLC column used was a 250 \times 2-mm Synergi Max RP C₁₂ column (Phenomenex, Torrance, CA). The mobile phase consisted of Solvent A, 0.1% (v/v) formic acid in water, and Solvent B, acetonitrile containing 0.1% (v/v) formic acid. The flow rate was 0.2 ml/min. A linear solvent gradient was used, running from 20 to 50% B in 10 min, 50 to 90% B over the next 2 min, held constant at 90% B for 7 min, returned to 20% B over 1 min, and equilibrated at 20% B for 5 min. For analysis of cotinine, the HPLC column used was a 150 \times 2-mm Synergi Hydro RP C₁₈ column (Phenomenex). The mobile phase consisted of Solvent A, 0.1% (v/v) formic acid in water, and Solvent B, acetonitrile containing 0.1% (v/v) formic acid. The flow rate was 0.2 ml/min. Separations were carried out by isocratic elution at 5% B with a run time of 5 min. Cotinine eluted at 2.33 min.

Table 2

LC-MS/MS properties of ONE and HNE metabolites detected in the urine of human smokers and nonsmokers

Analyte	MW	SRM Transition	Collision energy (eV)	Retention Time (min)	Figure	Concentration (nM) ^b
ONE-MA	317	316 \rightarrow 162	25	Peak not found		
ONE-MA-d ₃	320	319 \rightarrow 165	25	Peak not found		
HNE-MA	319	318 \rightarrow 189 ^a	25	10.5, 10.8	2	7.4–225
		318 \rightarrow 171	25	10.5, 10.8		
HNE-MA-d ₃	322	321 \rightarrow 189	25	10.5, 10.8		
		321 \rightarrow 171	25	10.5, 10.8		
ONO-MA	319	318 \rightarrow 162 ^a	25	11.3	2	1.7–177
ONO-MA-d ₃	322	321 \rightarrow 165	25	11.3		
DHN-MA	321	320 \rightarrow 191 ^a	25	9.8	2, 3	6.6–316
		320 \rightarrow 143	25	9.8		
DHN-MA-d ₃	324	323 \rightarrow 191	25	9.8		
		323 \rightarrow 143	25	9.8		
ONA-MA	333	332 \rightarrow 169	25	12.2	2	
		332 \rightarrow 162	25	12.2		
ONA-MA-d ₃	336	335 \rightarrow 169	25	12.2		
		335 \rightarrow 162	25	12.2		
HNA-MA	335	334 \rightarrow 162	25	10.2	2	
		334 \rightarrow 143	25	10.2		
HNA-MA-d ₃	338	337 \rightarrow 165	25	10.2		
		337 \rightarrow 143	25	10.2		
HNAL-MA	317	316 \rightarrow 162	25	13.2–13.6	2	
		316 \rightarrow 143	25	13.2–13.6		
HNAL-MA-d ₃	320	319 \rightarrow 165	25	13.2–13.6		
		319 \rightarrow 143	25	13.2–13.6		

^a Quantifying transition. Other transitions used as qualifiers.

^b Concentration is shown as a range encompassing the levels found for all study participants.

Mass spectrometry

An Applied Biosystems MDS Sciex hybrid triple quadrupole/linear ion trap mass spectrometer (4000 QTrap) equipped with a TurboV electrospray source (Concord, Canada) was used for these analyses. The TurboV source was maintained at 400 °C. The ion-spray voltage was 4500 V and the declustering potential was 40 V. Nitrogen was used as the source gas, curtain gas, and collision gas. Various scanning techniques, all run in negative ion mode, were used for the characterization and detection of LPO-MA products, including Q1, product ion scanning, and selected reaction monitoring (SRM). All SRM transitions and collision energies for the LPO-MA conjugates are shown in Table 2. SRM in positive ion mode was used for the quantitation of cotinine. The transitions used were m/z 177 → 80 as the quantifier and m/z 177 → 98 as the qualifier.

Data analysis

Peak area analysis was performed using Analyst 1.4.1 (Applied Biosystems). Analyte peak areas were normalized for the internal standard peak area, a 2-fold sample concentration, and for the creatinine concentration in milligrams per milliliter. Thus, all data are represented as milligrams per gram creatinine unless otherwise stated. The standard addition curve samples were concentrated 5-fold during sample preparation and this was taken into account for the calculation of endogenous metabolite levels using these curves. LPO-MA is the sum of HNE-MA, DHN-MA, and ONO-MA concentrations represented as milligrams per gram creatinine. Statistical comparisons were performed with GraphPad (San Diego, CA) using a paired or unpaired Student's *t* test as appropriate. Data are shown either as a range of concentrations or as mean ± SD.

Results

Quantitation of LPO products in human urine

We have developed an LC-MS/MS method for the simultaneous quantitation of HNE-MA, ONO-MA, and DHN-MA in human urine. Previous human studies have focused only on the quantitation of DHN-MA [22]. A study in rats by Mally et al. [26] quantified both HNE-MA and DHN-MA; however, they did not account for ONO-MA in their analysis.

Quantitation of HNE-MA

A calibration curve was constructed, using standard solutions containing varying concentrations of HNE-MA and a fixed concentration of HNE-MAD₃ (1.0 μM) as the internal standard. We also prepared a standard addition curve in order to assess the accuracy of our method and to investigate the possibility of matrix effects. Urine aliquots were spiked with a fixed amount of internal standard (10 μl of a 10 μM solution) and varying amounts (0.5–5.0 μM) of HNE-MA. Both curves were analyzed by LC-MS/MS (Fig. 1A). Extrapolation of the standard addition curve ($R^2 \geq 0.998$) to $y=0$ gave a sample concentration of 910 nM HNE-MA. However, it was also necessary to account for the concentration (5×) of the sample during preparation. Thus, the calculated 910 nM concentration divided by 5 gave the endogenous urinary HNE-MA concentration of 182 nM. This urinary concentration, calculated by the standard addition method, corresponded to a concentration of 203 ± 4.5 nM HNE-MA in aliquots ($n=3$) of the same urine sample calculated using the calibration curve ($R^2 \geq 0.998$, Fig. 1A). The lower limit of quantitation was determined to be 5 nM ($S/N=10$) for these analyses, allowing for detection of 2.5 nM concentrations of HNE-MA since smoker and nonsmoker samples were concentrated 2× during sample preparation.

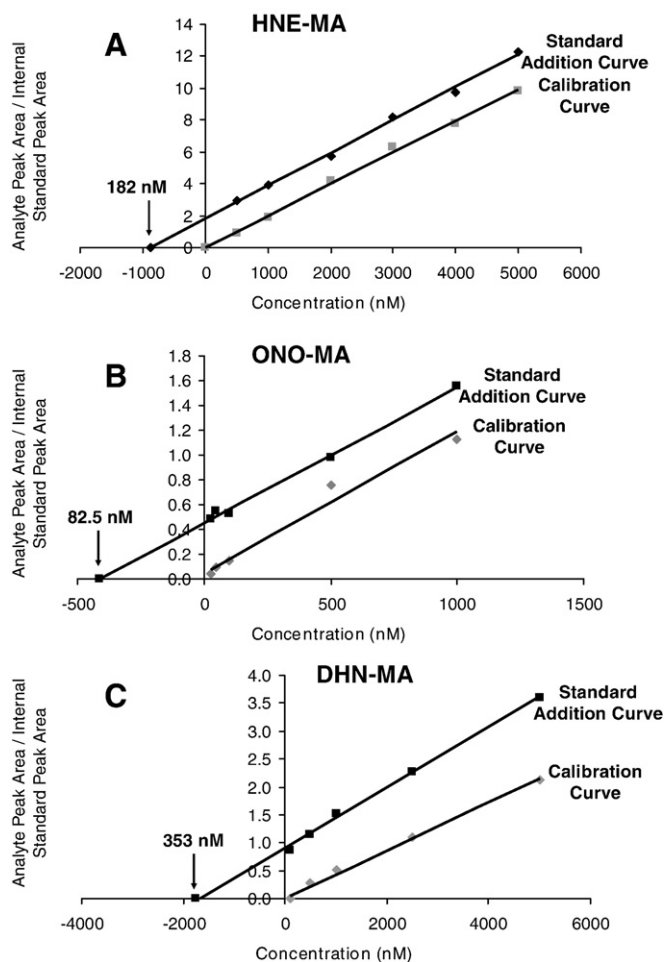


Fig. 1. Calibration curve and standard addition curve plots for HNE-MA (A), ONO-MA (B), and DHN-MA (C). The calibration curves were derived from the analysis of synthetic standards ranging in concentration from 0.5 to 5.0 μM for HNE-MA, 0.25 to 1.0 μM for ONO-MA, and 0.1 to 5.0 μM for DHN-MA. All curves were constructed using a fixed concentration of internal standard (1.0 μM HNE-MAD₃, 1.0 μM ONO-MAD₃, and 5.0 μM DHN-MAD₃). The standard addition curves were prepared by spiking 1.0-ml aliquots of urine with a fixed amount of internal standard and known amounts of LPO-MA conjugate. Samples were concentrated five times during preparation. Extrapolation of the standard addition curve to $y=0$ and division by 5 to account for concentration of the sample during preparation, gave endogenous urinary concentrations of 182 nM HNE-MA, 82.5 nM of ONO-MA, and 353 nM of DHN-MA.

Validation of HNE-MA standard

A HNE-MA standard (1 mg in 100 μl ethanol) was purchased from Cayman Chemical for use to validate the concentration of our synthetically prepared material. In order to do this, a calibration curve was prepared using varying amounts (0.5–5.0 μM) of the Cayman HNE-MA standard and a fixed amount of HNE-MAD₃ (10 μl of a 10 μM solution). This curve was analyzed by LC-MS/MS and compared to the calibration curve prepared using HNE-MA synthesized in our lab. The curve prepared from HNE-MA prepared in our lab had a slope of 0.0020 and $R^2 \geq 0.997$, while the Cayman HNE-MA resulted in a curve with a slope of 0.0023 and $R^2 \geq 0.994$, demonstrating that our method of HNE-MA synthesis provided results comparable to those obtained with the commercial material.

Quantitation of ONO-MA

Varying concentrations of ONO-MA and a fixed concentration of internal standard ONO-MAD₃ (1.0 μM) were used to prepare a calibration curve. A standard addition curve was also prepared by spiking urine aliquots with a fixed amount of internal standard (10 μl

of a 10 μM solution) and varying concentrations of ONO-MA (0.25–1.0 μM). Both curves were analyzed by LC-MS/MS (Fig. 1B). Extrapolation of the standard addition curve ($R^2 \geq 0.998$) to $y=0$ (calculated concentration 412.5 nM) and accounting for sample concentration (5 \times) gave an endogenous ONO-MA concentration of 82.5 nM. This urinary concentration, calculated by the standard addition method, corresponded to a concentration of 67.1 ± 7.9 nM ONO-MA in aliquots ($n=3$) of the same urine sample analyzed using the calibration curve ($R^2 \geq 0.975$, Fig. 1B). The lower limit of quantitation was determined to be 0.5 nM ($S/N=10$) for these analyses, allowing for detection of 0.25 nM concentrations of ONO-MA since smoker and nonsmoker samples were concentrated 2 \times during sample preparation.

Quantitation of DHN-MA

A calibration curve was constructed, using varying amounts of DHN-MA and a fixed amount of DHN-MA $_d_3$ (5.0 μl of a 100 μM solution) as the internal standard. We also prepared a standard addition curve, spiking urine aliquots with a fixed amount of internal standard (5.0 μl of a 100 μM solution) and varying concentrations of DHN-MA (0.1–5.0 μM). Both curves were analyzed by LC-MS/MS (Fig. 1C). Extrapolation of the standard addition curve ($R^2 \geq 0.998$) to $y=0$ (calculated concentration 1765 nM) and accounting for sample concentration (5 \times) gave an endogenous DHN-MA concentration of 353 nM. This urinary concentration, calculated by the standard addition method, corresponded to a concentration of 457 nM DHN-MA in an aliquot ($n=1$) of the same urine sample analyzed using the calibration curve ($R^2 \geq 0.996$, Fig. 1C). The lower limit of quantitation was determined to be 10 nM ($S/N=10$) for these analyses, allowing for detection of 5 nM concentrations of DHN-MA since samples were concentrated 2 \times during sample preparation.

Stability of standards

The LPO-MA conjugate solutions used in this study were generally found to be stable over a period of 6 months when stored at -20 $^\circ\text{C}$. HNA-MA is the one exception since it spontaneously converts to HNAL-MA and should be prepared fresh every few weeks. We found it best to assess the standards and internal standards by LC-MS/MS each

time a batch of samples was run to ensure that the levels remained consistent over time, preparing new standards from the LPO product and MA if necessary.

LPO products in human urine

The LPO products, HNE-MA, DHN-MA, HNA-MA, HNAL-MA, ONO-MA, and ONA-MA, were all detected in human urine samples (Fig. 2). We were not able to quantify HNA-MA, HNAL-MA, and ONA-MA in human urine. The endogenous amounts of ONA-MA, estimated at <10 nM, were too small to quantify by isotope-dilution LC-MS/MS with satisfactory precision and accuracy. HNA-MA and HNAL-MA presented a different challenge. Due to the spontaneous conversion of HNA-MA into HNAL-MA under aqueous conditions, we have thus far been unable to obtain homogenous synthetic standards of either material for use in our calibration curves.

ONE-MA

It should be noted that while we have previously demonstrated the presence of ONE-MA in rat urine [20], it was not detectable in our human urine samples. Its absence in human urine is likely due to preferential phase I metabolism of ONE or ONE-GSH resulting in metabolites ONO-MA and ONA-MA. ONE is also able to covalently modify cysteine, histidine, and lysine residues in proteins [27,28], making it undetectable by our methods. Moreover, the GSH conjugate of ONE retains its ability to undergo Schiff base formation. It is also possible that thiadiazabicyclo-ONE-glutathione (TOG), a metabolite of ONE in cultured endothelial (EA.hy 926) cells [29], is formed *in vivo*. The formation of TOG involves cyclization of the γ -glutamic acid residue of ONE-GSH, preventing further metabolism of the GSH moiety to form ONE-MA. TOG formation is likely a minor pathway, however, since we are able to quantify ONO-MA levels and to detect ONA-MA in the human urine samples.

Metabolite confirmation

Enhanced product ion (EPI) scanning, along with the comparison of biological samples to synthetic standards prepared in our lab, was used to ensure correct metabolite identification. EPI was performed by

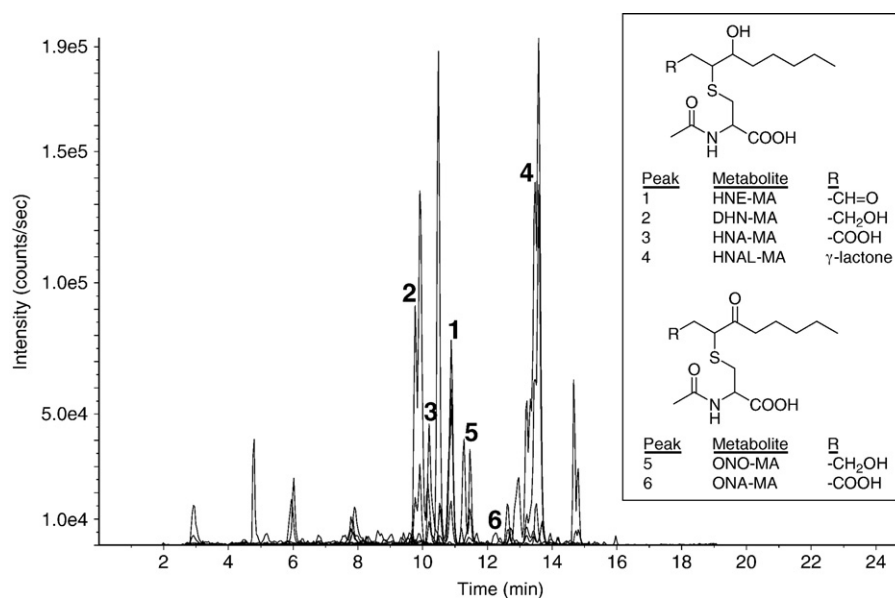


Fig. 2. LC-SRM chromatogram of a human urine sample. Key to chromatographic peaks: (1) HNE-MA m/z 318 \rightarrow 189 and m/z 318 \rightarrow 171; (2) DHN-MA m/z 320 \rightarrow 191 and m/z 320 \rightarrow 143; (3) HNA-MA m/z 334 \rightarrow 162; (4) HNAL-MA m/z 316 \rightarrow 162 and m/z 316 \rightarrow 143; (5) ONO-MA m/z 318 \rightarrow 162; (6) ONA-MA m/z 332 \rightarrow 169 and m/z 332 \rightarrow 162. ONE-MA was not detected.

selecting a m/z of interest in Q1, inducing fragmentation in Q2, and then utilizing the linear ion trap mode to trap these fragments in Q3, followed by Q3 scanning in quadrupole mode. This technique allows for the sensitive MS/MS comparison of analytes in synthetic and biological samples. Fig. 3 shows EPI spectra in negative ion mode for synthetic and biological DHN-MA, which eluted at 9.8 min (Figs. 3A and 3C). Both of these samples demonstrate that DHN-MA produces fragments with m/z 191 and m/z 143, both β -elimination fragments, and m/z 173, formed via a McLafferty rearrangement (Figs. 3B and 3D). Similar experiments were performed for HNE-MA and ONO-MA in our previous work [20].

Smoking cessation

Smoking cessation caused significant decreases in the urinary levels of HNE-MA, DHN-MA, and LPO-MA present in a group of seven human subjects (Fig. 4). There was no significant change in any of these metabolites over the same time period in nonsmoking subjects (paired Student's t test, $P > 0.05$). We also did not find any significant differences in metabolite levels between the smoker and the nonsmoker groups prior to or following cessation (unpaired Student's t test, $P > 0.05$). Neither did we find any significant correlation between LPO-MA and age ($P = 0.88$) or BMI ($P = 0.35$). All calculations included normalization for creatinine levels to account for variation in urine concentration between individuals. There was no significant difference in the urinary creatinine levels before and after smoking cessation ($P = 0.45$).

Discussion

A semiquantitative method for analysis of HNE-MA and ONE-MA metabolites in the urine of oxidatively stressed rats was previously reported [20]. While this method allowed for the simultaneous analysis of multiple LPO-MA conjugates, the data were not quantitative. Appropriate internal standards for each of our analytes of interest are necessary in order to perform absolute quantitation. We first

synthesized MA_3 following the method of Slatter et al. [25]. MA_3 conjugates of HNE, DHN, HNA, ONE, ONO, and ONA, were then prepared as described by Kuiper et al. [20]. Quantitation of endogenous LPO-MA conjugates was subsequently achieved by isotope-dilution LC-MS/MS using SRM. We now demonstrate, for the first time, the quantitative determination of ONO-MA in addition to HNE-MA and DHN-MA *in vivo* at low milligram per gram creatinine levels.

In smokers and nonsmokers, we found that the urinary levels of ONO-MA were in the range 0.05–2.26 mg/g creatinine (1.7–177 nM). HNE-MA was present in the range of 0.17–12.19 mg/g creatinine (7.4–225 nM) and DHN-MA at levels of 0.22–17.90 mg/g creatinine (6.6–316 nM). Low LPO-MA conjugate levels in a subgroup of the smokers resulted in the lack of statistical difference between the smoker and the nonsmoker groups prior to smoking cessation. Alary et al. [22] also assessed DHN-MA in humans and found production of 5 $\mu\text{g}/24$ h in seven healthy human volunteers, which corresponds to 2.7 ng/ml (8.4 nM). These levels are comparable to the low levels of DHN-MA in our study. In a study of the urinary excretion of LPO-MA conjugates in rats, Mally et al. [26] measured 113.8 ± 36.8 pmol/mg creatinine for HNE-MA (36 $\mu\text{g}/\text{g}$ creatinine) and 1.19 ± 0.33 nmol/mg creatinine for DHN-MA (382 $\mu\text{g}/\text{g}$ creatinine). Rathahao et al. [21] and Guéraud et al. [23] found urinary production of DHN-MA in rats to be in the range of 45–230 ng/24 h (equivalent to 8.8–45 nM, assuming a urine production of 16 ml/24 h), with the higher concentrations appearing in BrCCl_3 -stressed animals. Alary et al. [22] also analyzed rat urine and found DHN-MA production of 10 ng/24 h or 0.8 ng/ml (2.5 nM). Urinary levels of DHN-MA in lean and Zucker obese rats (1.1 and 2.9 μM , respectively), reported by Orioli et al. [24], however, are much higher than the other reported values. With the exception of the levels reported by Orioli et al. [24], urinary levels of HNE-MA and DHN-MA in rats seem to be lower than or at the low end of the range of human levels determined in Alary's study [22] and in our present study. Since the urinary levels of LPO-MA conjugates in rats tend to fall within the same range as the levels we found in human samples, our quantitation method should be applicable to animal investigations as well.

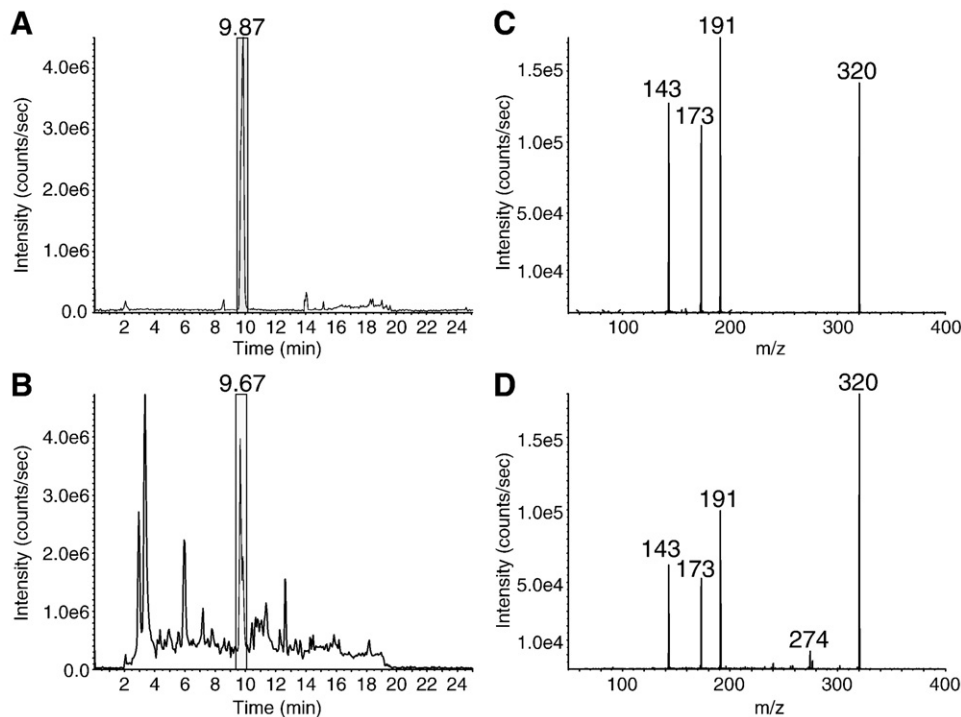


Fig. 3. LC-EPI chromatograms of a DHN-MA synthetic standard and a human urine sample. (A) Negative ion electrospray EPI scanning of m/z 320 of a standard reaction mixture of DHN-MA. (B) Negative ion electrospray EPI scanning of m/z 320 of a human urine sample. (C) The EPI spectrum of synthetic DHN-MA shows fragments with m/z 191, m/z 143, and m/z 173. (D) The EPI spectrum of endogenous DHN-MA in a human urine sample shows the same fragments as the synthetic DHN-MA sample, with m/z 191, m/z 143, and m/z 173.

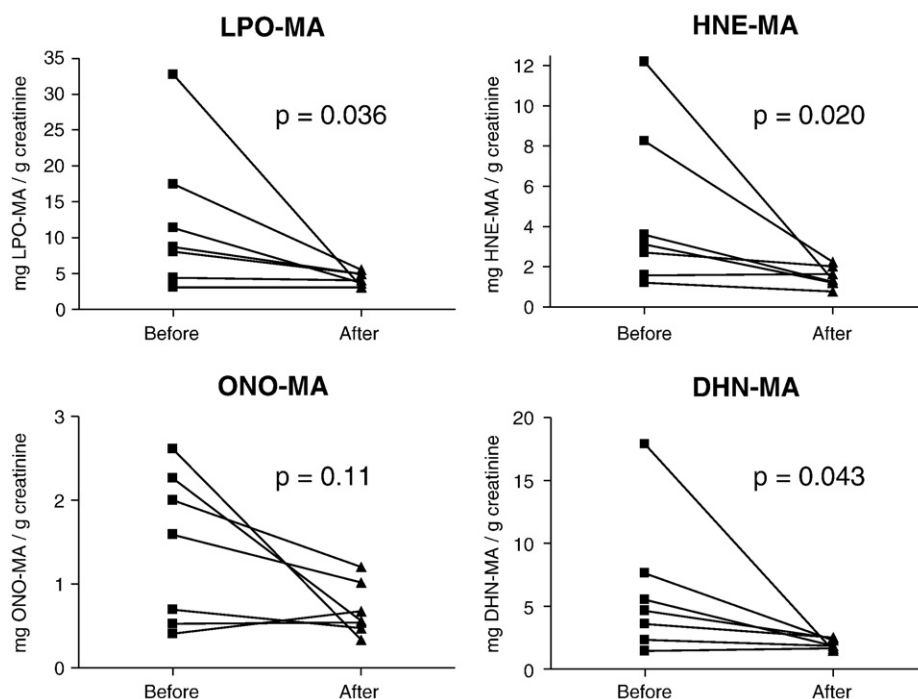


Fig. 4. Comparison of LPO metabolites in smokers before and after smoking cessation. HNE-MA, DHN-MA, and LPO-MA were significantly decreased after 12 weeks of smoking cessation in humans with *P* values of 0.020, 0.043, and 0.036, respectively. LPO-MA is the sum of HNE-MA, DHN-MA, and ONO-MA. Data were analyzed on a logarithmic scale.

Like HNE and ONE, $F_{2\alpha}$ -isoprostanes are formed from lipid hydroperoxides via radical-mediated pathways. $F_{2\alpha}$ -isoprostanes are generally considered to be the most reliable markers of *in vivo* oxidative stress [30,31]. Smoking cessation has been shown to result in significant decreases of urinary $F_{2\alpha}$ -isoprostane levels after 1 or 2 weeks [32,33]. The study conducted by Chehne et al. [33] demonstrated that the decrease of urinary $F_{2\alpha}$ -isoprostane levels on smoking cessation was similar between patients having clinically manifested atherosclerosis with or without hypercholesterolemia and/or hypertension, indicating that cigarette smoke is a major contributor to *in vivo* oxidative stress compared to other risk factors of atherosclerosis. Similar to urinary $F_{2\alpha}$ -isoprostane levels, our study of apparently healthy participants showed significant decreases in the levels of MA conjugates of HNE and DHN in the urine upon smoking cessation, reflecting a similar pathway of formation via lipid hydroperoxides.

The LPO metabolites of our study differ from the $F_{2\alpha}$ -isoprostanes in that they are also products of phase I and phase II metabolism. Thus, the levels of MA conjugates of HNE, DHN, and ONO reflect both the formation of HNE and ONE and their subsequent metabolism. Expression levels of GSTs may therefore codetermine urinary levels of HNE-MA, DHN-MA, and ONO-MA. GSTP1, a GST isoenzyme involved in HNE conjugation [34,35], was induced in lung tissue of smokers whereas other GSTs, GSTA2, and GSTM1 showed no difference in expression levels between smokers and nonsmokers [36]. On the other hand, genetic polymorphisms of GST may affect gene expression if the mutation is located in the promoter region. Qian et al. [37] studied single nucleotide polymorphisms (SNPs) of GSTA4, another GST that accepts HNE as a substrate [38]. Qian et al. [37] found that the presence of genotypes TA and AA at locus -1718 of GSTA4 was associated with a 37% significantly decreased risk of lung cancer compared to the TT genotype. The authors suggested that the TA and AA genotypes, with the SNP in the promoter region, may have increased GSTA4 expression and thus greater capacity to detoxify HNE as compared to the TT genotype. Dwivedi et al. [39] determined that GSTA4 null mice have higher levels of hepatic HNE after CCl_4 treatment than wild-type mice, indicating reduced HNE conjugation

in GSTA4 null mice. In the study by Qian et al. [40], the TT genotype had a prevalence of 77% in lung cancer patients ($n = 500$) and 68% in cancer-free control subjects ($n = 517$). The common occurrence of the TT genotype, presumably having reduced GSTA4 expression and reduced capacity to conjugate HNE, may explain the low urinary levels of LPO-MA (<7 mg/g creatinine) we found in 9 out of 23 smokers.

The low LPO-MA excretion in nine smokers may also be due to smoking-induced phase I metabolism, resulting in enhanced conversion of HNE and ONE into DHN which is not a GST substrate. Aldo-keto reductase 1B10 (AKR1B10) is known to reduce HNE to DHN and to reduce ONE to ONO [41]. Its up-regulation in smokers, shown by Fukumoto et al. [42] and Nagaraj et al. [43], would direct the metabolism of HNE to DHN, resulting in decreased formation of GST-mediated metabolites and MA conjugates (Scheme 1).

We developed a method for the accurate quantitation of ONO-MA, HNE-MA, and DHN-MA in human urine by isotope-dilution LC-MS/MS. We also detected HNA-MA, HNAL-MA, and ONA-MA. The significance of the *in vivo* detection of ONO-MA and ONA-MA is that these conjugates represent HNE/ONE branching in the breakdown of lipid hydroperoxides as shown in Scheme 1, suggesting that ONO may contribute to the deleterious effects previously ascribed to HNE. Our findings also show that LPO-MA conjugates are elevated in urine obtained from smokers and decrease significantly following smoking cessation, demonstrating the utility of these metabolites as markers of *in vivo* oxidative stress.

Acknowledgments

This work was supported in part by the National Institutes of Health (R01HL081721, S10RR022589, and P30ES000210), an OSU Center for Healthy Aging Research Fellowship, a grant from the John C. Erkkila, MD, Endowment for Health and Human Performance, and by a donation from the estate of Leland J. Gross. We thank pharmacy residents Rachelle Collier and Tiffany Boehland for teaching smoking cessation classes to the smokers enrolled in the study.

References

- [1] Benedetti, A.; Comporti, M.; Esterbauer, H. Identification of 4-hydroxynonenal as a cytotoxic product originating from the peroxidation of liver microsomal lipids. *Biochim. Biophys. Acta* **620**:281–296; 1980.
- [2] Esterbauer, H.; Schaur, R. J.; Zollner, H. Chemistry and biochemistry of 4-hydroxynonenal, malonaldehyde and related aldehydes. *Free Radic. Biol. Med.* **11**: 81–128; 1991.
- [3] Barbin, A. Formation of DNA etheno adducts in rodents and humans and their role in carcinogenesis. *Acta Biochim. Pol.* **45**:145–161; 1998.
- [4] Spiteller, G. The important role of lipid peroxidation processes in aging and age dependent diseases. *Mol. Biotechnol.* **37**:5–12; 2007.
- [5] Facchinetti, F.; Amadei, F.; Geppetti, P.; Tarantini, F.; Di Serio, C.; Dragotto, A.; Gigli, P. M.; Catinella, S.; Civelli, M.; Patacchini, R. Alpha,beta-unsaturated aldehydes in cigarette smoke release inflammatory mediators from human macrophages. *Am. J. Respir. Cell Mol. Biol.* **37**:617–623; 2007.
- [6] Rahman, I.; van Schadewijk, A. A.; Crowther, A. J.; Hiemstra, P. S.; Stolk, J.; MacNee, W.; De Boer, W. I. 4-Hydroxy-2-nonenal, a specific lipid peroxidation product, is elevated in lungs of patients with chronic obstructive pulmonary disease. *Am. J. Respir. Crit. Care Med.* **166**:490–495; 2002.
- [7] Butterfield, D. A.; Sultana, R. Redox proteomics identification of oxidatively modified brain proteins in Alzheimer's disease and mild cognitive impairment: insights into the progression of this dementing disorder. *J. Alzheimers Dis.* **12**: 61–72; 2007.
- [8] Lovell, M. A.; Markesbery, W. R. Oxidative DNA damage in mild cognitive impairment and late-stage Alzheimer's disease. *Nucleic Acids Res.* **35**:7497–7504; 2007.
- [9] Picklo, M. J. S.; Montine, T. J. Mitochondrial effects of lipid-derived neurotoxins. *J. Alzheimers Dis.* **12**:185–193; 2007.
- [10] Mitchell, D. Y.; Petersen, D. R. The oxidation of alpha-beta unsaturated aldehyde products of lipid peroxidation by rat liver aldehyde dehydrogenases. *Toxicol. Appl. Pharmacol.* **87**:403–410; 1987.
- [11] Doorn, J. A.; Hurley, T. D.; Petersen, D. R. Inhibition of human mitochondrial aldehyde dehydrogenase by 4-hydroxynon-2-enal and 4-oxonon-2-enal. *Chem. Res. Toxicol.* **19**:102–110; 2006.
- [12] Srivastava, S.; Dixit, B. L.; Cai, J.; Sharma, S.; Hurst, H. E.; Bhatnagar, A.; Srivastava, S. K. Metabolism of lipid peroxidation product, 4-hydroxynonenal (HNE) in rat erythrocytes: role of aldose reductase. *Free Radic. Biol. Med.* **29**:642–651; 2000.
- [13] Jian, W.; Arora, J. S.; Oe, T.; Shuvaev, V. V.; Blair, I. A. Induction of endothelial cell apoptosis by lipid hydroperoxide-derived bifunctional electrophiles. *Free Radic. Biol. Med.* **39**:1162–1176; 2005.
- [14] Doorn, J. A.; Srivastava, S. K.; Petersen, D. R. Aldose reductase catalyzes reduction of the lipid peroxidation product 4-oxonon-2-enal. *Chem. Res. Toxicol.* **16**: 1418–1423; 2003.
- [15] Blair, I. A. Endogenous glutathione adducts. *Curr. Drug Metab.* **7**:853–872; 2006.
- [16] Agianian, B.; Tucker, P. A.; Schouten, A.; Leonard, K.; Bullard, B.; Gros, P. Structure of a Drosophila sigma class glutathione S-transferase reveals a novel active site topography suited for lipid peroxidation products. *J. Mol. Biol.* **326**:151–165; 2003.
- [17] Knoll, N.; Ruhe, C.; Veeriah, S.; Sauer, J.; Gleit, M.; Gallagher, E. P.; Pool-Zobel, B. L. Genotoxicity of 4-hydroxy-2-nonenal in human colon tumor cells is associated with cellular levels of glutathione and the modulation of glutathione S-transferase A4 expression by butyrate. *Toxicol. Sci.* **86**:27–35; 2005.
- [18] Gallagher, E. P.; Huisden, C. M.; Gardner, J. L. Transfection of HepG2 cells with hGSTA4 provides protection against 4-hydroxynonenal-mediated oxidative injury. *Toxicol. In Vitro* **21**:1365–1372; 2007.
- [19] Alary, J.; Bravais, F.; Cravedi, J. P.; Debrauwer, L.; Rao, D.; Bories, G. Mercapturic acid conjugates as urinary end metabolites of the lipid peroxidation product 4-hydroxy-2-nonenal in the rat. *Chem. Res. Toxicol.* **8**:34–39; 1995.
- [20] Kuiper, H. C.; Miranda, C. L.; Sowell, J. D.; Stevens, J. F. Mercapturic acid conjugates of 4-hydroxy-2-nonenal and 4-oxo-2-nonenal metabolites are in vivo markers of oxidative stress. *J. Biol. Chem.* **283**:17131–17138; 2008.
- [21] Rathahao, E.; Peiro, G.; Martins, N.; Alary, J.; Guéraud, F.; Debrauwer, L. Liquid chromatography-multistage tandem mass spectrometry for the quantification of dihydroxynonene mercapturic acid (DHN-MA), a urinary end-metabolite of 4-hydroxynonenal. *Anal. Bioanal. Chem.* **381**:1532–1539; 2005.
- [22] Alary, J.; Debrauwer, L.; Fernandez, Y.; Cravedi, J. P.; Rao, D.; Bories, G. 1,4-Dihydroxynonene mercapturic acid, the major end metabolite of exogenous 4-hydroxy-2-nonenal, is a physiological component of rat and human urine. *Chem. Res. Toxicol.* **11**:130–135; 1998.
- [23] Guéraud, F.; Peiro, G.; Bernard, H.; Alary, J.; Créminon, C.; Debrauwer, L.; Rathahao, E.; Drumare, M. F.; Canlet, C.; Wal, J. M.; Bories, G. Enzyme immunoassay for a urinary metabolite of 4-hydroxynonenal as a marker of lipid peroxidation. *Free Radic. Biol. Med.* **40**:54–62; 2006.
- [24] Orioli, M.; Aldini, G.; Benfatto, M. C.; Facino, R. M.; Carini, M. HNE Michael adducts to histidine and histidine-containing peptides as biomarkers of lipid-derived carbonyl stress in urines: LC-MS/MS profiling in Zucker obese rats. *Anal. Chem.* **79**: 9174–9184; 2007.
- [25] Slatter, J. G.; Rashed, M. S.; Pearson, P. G.; Han, D. H.; Baillie, T. A. Biotransformation of methyl isocyanate in the rat. Evidence for glutathione conjugation as a major pathway of metabolism and implications for isocyanate-mediated toxicities. *Chem. Res. Toxicol.* **4**:157–161; 1991.
- [26] Mally, A.; Amberg, A.; Hard, G. C.; Dekant, W. Are 4-hydroxy-2(E)-nonenal derived mercapturic acids and (1)H NMR metabolomics potential biomarkers of chemically induced oxidative stress in the kidney? *Toxicology* **230**:244–255; 2007.
- [27] Zhang, W. H.; Liu, J.; Xu, G.; Yuan, Q.; Sayre, L. M. Model studies on protein side chain modification by 4-oxo-2-nonenal. *Chem. Res. Toxicol.* **16**:512–523; 2003.
- [28] Sayre, L. M.; Lin, D.; Yuan, Q.; Zhu, X.; Tang, X. Protein adducts generated from products of lipid oxidation: focus on HNE and ONE. *Drug Metab. Rev.* **38**:651–675; 2006.
- [29] Jian, W.; Lee, S. H.; Mesaros, C.; Oe, T.; Elipe, M. V.; Blair, I. A. A novel 4-oxo-2(E)-nonenal-derived endogenous thiadiazabicyclo glutathione adduct formed during cellular oxidative stress. *Chem. Res. Toxicol.* **20**:1008–1018; 2007.
- [30] Basu, S. F2-isoprostanes in human health and diseases: from molecular mechanisms to clinical implications. *Antioxid. Redox Signal.* **10**:1405–1434; 2008.
- [31] Montuschi, P.; Barnes, P.; Roberts 2nd, L. J. Insights into oxidative stress: the isoprostanes. *Curr. Med. Chem.* **14**:703–717; 2007.
- [32] Pilz, H.; Oguogho, A.; Chehne, F.; Lupattelli, G.; Palumbo, B.; Sinzinger, H. Quitting cigarette smoking results in a fast improvement of in vivo oxidation injury (determined via plasma, serum and urinary isoprostane). *Thromb. Res.* **99**:209–221; 2000.
- [33] Chehne, F.; Oguogho, A.; Lupattelli, G.; Palumbo, B.; Sinzinger, H. Effect of giving up cigarette smoking and restarting in patients with clinically manifested atherosclerosis. *Prostaglandins Leukot. Essent. Fatty Acids* **67**:333–339; 2002.
- [34] Gallagher, E. P.; Gardner, J. L.; Barber, D. S. Several glutathione S-transferase isozymes that protect against oxidative injury are expressed in human liver mitochondria. *Biochem. Pharmacol.* **71**:1619–1628; 2006.
- [35] Hayes, J. D.; Flanagan, J. U.; Jowsey, I. R. Glutathione transferases. *Annu. Rev. Pharmacol. Toxicol.* **45**:51–88; 2005.
- [36] Thum, T.; Erpenbeck, V. J.; Moeller, J.; Hohlfeld, J. M.; Krug, N.; Borlak, J. Expression of xenobiotic metabolizing enzymes in different lung compartments of smokers and nonsmokers. *Environ. Health Perspect.* **114**:1655–1661; 2006.
- [37] Qian, J.; Jing, J.; Jin, G.; Wang, H.; Wang, Y.; Liu, H.; Wang, H.; Li, R.; Fan, W.; An, Y.; Sun, W.; Wang, Y.; Ma, H.; Miao, R.; Hu, Z.; Jin, L.; Wei, Q.; Shen, H.; Huang, W.; Lu, D. Association between polymorphisms in the GSTA4 gene and risk of lung cancer: a case-control study in a Southeastern Chinese population. *Mol. Carcinog.* **48**: 253–259; 2009.
- [38] Hubatsch, I.; Ridderstrom, M.; Mannervik, B. Human glutathione transferase A4-4: an alpha class enzyme with high catalytic efficiency in the conjugation of 4-hydroxynonenal and other genotoxic products of lipid peroxidation. *Biochem. J.* **330** (Pt 1):175–179; 1998.
- [39] Dwivedi, S.; Sharma, R.; Sharma, A.; Zimniak, P.; Ceci, J. D.; Awasthi, Y. C.; Boor, P. J. The course of CCl4 induced hepatotoxicity is altered in mGSTA4-4 null (-/-) mice. *Toxicology* **218**:58–66; 2006.
- [40] Qian, J.; Jing, J.; Jin, G.; Wang, H.; Wang, Y.; Liu, H.; Wang, H.; Li, R.; Fan, W.; An, Y.; Sun, W.; Wang, Y.; Ma, H.; Miao, R.; Hu, Z.; Jin, L.; Wei, Q.; Shen, H.; Huang, W.; Lu, D. Association between polymorphisms in the GSTA4 gene and risk of lung cancer: a case-control study in a Southeastern Chinese population. *Mol. Carcinog.* **48**: 253–259; 2009.
- [41] Martin, H. J.; Maser, E. Role of human aldo-keto-reductase AKR1B10 in the protection against toxic aldehydes. *Chem. Biol. Interact.* **178**:145–150; 2009.
- [42] Fukumoto, S.; Yamauchi, N.; Moriguchi, H.; Hippi, Y.; Watanabe, A.; Shibahara, J.; Taniguchi, H.; Ishikawa, S.; Ito, H.; Yamamoto, S.; Iwanari, H.; Hironaka, M.; Ishikawa, Y.; Niki, T.; Sahara, Y.; Kodama, T.; Nishimura, M.; Fukayama, M.; Dosaka-Akita, H.; Aburatani, H. Overexpression of the aldo-keto reductase family protein AKR1B10 is highly correlated with smokers' non-small cell lung carcinomas. *Clin. Cancer Res.* **11**:1776–1785; 2005.
- [43] Nagaraj, N. S.; Beckers, S.; Mensah, J. K.; Waigel, S.; Vigneswaran, N.; Zacharias, W. Cigarette smoke condensate induces cytochromes P450 and aldo-keto reductases in oral cancer cells. *Toxicol. Lett.* **165**:182–194; 2006.